# Optimising the ITER 15MA DT Baseline Scenario by Exploiting a Self-Consistent Free-Boundary Core-edge-SOL Workflow in IMAS

F. Köchl<sup>1</sup>, S. D. Pinches<sup>2</sup>, C. Bourdelle<sup>3</sup>, F. J. Casson<sup>1</sup>, J. Citrin<sup>4</sup>, G. Corrigan<sup>1</sup>, M. Dubrov<sup>5</sup>, Y. Gribov<sup>2</sup>, D. Harting<sup>1</sup>, A. A. Kavin<sup>6</sup>, R. R. Khayrutdinov<sup>5</sup>, S.-H. Kim<sup>2</sup>, P. J. Knight<sup>1</sup>, S. V. Konovalov<sup>5</sup>, A. Loarte<sup>1</sup>, V. E. Lukash<sup>5</sup>, M. Marin<sup>4</sup>, S. Medvedev<sup>7</sup>, V. Parail<sup>1</sup>, A. R. Polevoi<sup>2</sup>, M. Romanelli<sup>1</sup>

EUROfusion Consortium, JET, Culham Science Centre, Abingdon, OX14 3DB, UK

<sup>1</sup>Culham Centre for Fusion Energy, Culham Science Centre, Abingdon, OX14 3DB, UK

<sup>2</sup>ITER Organization, Route de Vinon-sur-Verdon, CS 90 046,

13067 St Paul Lez Durance Cedex, France.

<sup>3</sup>CEA, IRFM, F-13108 Saint Paul-lez-Durance, France.

<sup>4</sup>DIFFER-Dutch Institute for Fundamental Energy Research, De Zaale 20, 5612 AJ

Eindhoven, Netherlands.

<sup>5</sup>National Research Centre "Kurchatov Institute", Moscow, Russia. <sup>6</sup>Joint Stock Company Efremov Institute, Saint Petersburg, Russia. <sup>7</sup>Keldysh Institute of Applied Mathematics, Moscow, Russia.

E-mail: Florian.Koechl@ukaea.uk

**Abstract.** The ability to describe the essential physics and technology elements needed to robustly simulate the operation of ITER is critical to being able to model the plasma scenarios that will run in ITER. The DINA and JINTRAC codes embedded in the Integrated Modelling & Analysis Suite are used to simulate the 15 MA DT baseline scenario operation, including a description of the plasma evolution from its core up to the plasma facing components respecting the principal engineering limitations of the poloidal field (PF) coil system. It is demonstrated that the foreseen scenario could be executed respecting all operational constraints by optimisation of the scenario layout and control schemes for the plasma shape control, current induction, heating, fuelling and seeding actuators. In addition, it is shown by means of complementary simulations that the core contamination by medium-Z impurities due to seeding requirements may actually be beneficial for core confinement.

### 1. Introduction

For an accurate assessment of possible constraint violations and control capabilities of the foreseen ITER scenarios and for the development of optimised actuator strategies in order to increase plasma operation performance and reliability, the strong level of interaction and nonlinear dependencies between various physics processes at play in tokamak discharges requires an integrated modelling approach. In this approach, codes for the prediction of plasma geometry, shape and position stability control, MHD stability, heat, particle and momentum sources as well as core, edge and SOL transport and plasma-wall interactions are combined in a consistent manner. Due to the complexity of such schemes, efforts are required to ensure an efficient development, adaptation and execution of appropriate integrated modelling workflows. As such, the usage of standardised and automatised methods for the coupling and exchange of information between model components is highly desirable. In addition, workflows need to be prepared in a way so that, at the same time, a reasonably fast execution can be ensured while a high level of accuracy in the calculation can be ascertained.

Attempts have recently been made to fulfil all these requirements by integration of the free boundary equilibrium code DINA [Lukash PDO 2005, Lukash EPS 2011] with the JINTRAC suite of codes [Romanelli PFR 2014], exploiting their full core+edge+SOL+MHD modelling capabilities within the Integrated Modelling & Analysis Suite (IMAS) [Imbeaux NF 2015, Pinches FEC 2016] as an IMAS workflow in open loop coupling. For the first time, the 15 MA / 5.3 T DT ITER baseline scenario has been assessed for the entire evolution from the early ramp-up phase (from X-point formation) until the late ramp-down phase (X-point to limiter transition) by means of integrated simulations with consideration of core+edge and

core+edge+SOL transport of neutral and ionised particles, heat, momentum and current with time-dependent free boundary plasma geometry and with the pedestal pressure being determined by continuous self-consistent edge MHD stability analysis.

The IMAS open loop coupling scheme between DINA and JINTRAC is validated for the current ramp-up phase and shown to converge within a few iterations. Attempts are made in the first iterations to optimise the PF coil current, heating, fuelling and seeding control schemes to demonstrate that a robust execution of the baseline scenario discharge can be assured with plasma conditions being well within operational limits at all times.

The IMAS modelling scheme and simulation conditions are summarised in Section 2, followed by a presentation of benchmark results in Section 3. Complete scenario calculations from the early ramp-up to the late ramp-down phase including optimisation attempts in the first iterations and demonstrating convergence for the open loop coupling scheme are described in Section 4. First integrated free boundary core+edge+MHD and core+edge+SOL+MHD modelling results for phases of particular interest are shown and discussed in Sections 5 and 6, respectively. Section 7 deals with complementary core+edge transport calculations for the quasi-stationary baseline flat-top phase with the aim to investigate the effect of core medium-Z impurity contamination on core transport conditions and vice-versa, followed by a brief summary.

### 2. Simulation conditions

All simulations presented in this paper have been carried out by exploitation of the IMAS modelling platform with automatised exchange of boundary conditions between the DINA and JINTRAC codes via standardised IDS data structures. The DINA and JINTRAC IMAS drivers (for core+edge or core+edge+SOL transport) are executed consecutively with input and output for the prescription of boundary conditions retrieved from IDS output from the previous iteration. While the plasma boundary contour and SOL grid information as well as the total current that is imposed as boundary condition in the current diffusion equation from DINA are prescribed in JINTRAC, solutions for the kinetic and non-inductive current density profiles from JINTRAC are imposed in the DINA runs. The scenario calculations are repeated in an iterative approach within the IMAS framework until both codes converge on the same solution, notably for the equilibrium and safety factor. This weak coupling scheme in open loop is proven to be robust thanks to very simple interface requirements and perfect adherence to the constraint of q preservation in the adiabatic limit, and it is known to converge fast to the same solution that is obtained in close coupling schemes for transients that are slow, weak in amplitude, or that can be mitigated such as current ramp phases and regular transitions between L- and H-mode. It may therefore be well suitable for the fast and efficient full scenario modelling in scenario design and analysis studies for ITER.

In the DINA-JINTRAC IMAS modelling scheme, a new version of the DINA code is applied [Lukash EPS 2014] that allows the validation of the ITER PF system capability to support scenarios obtained with other codes such as JINTRAC, which may have more sophisticated plasma transport models, but do not have the capability of: 1) detailed simulation of plasma magnetic control, 2) correct calculation of the magnetic flux in absolute terms that is linked with the plasma and 3) detailed integration of all engineering limitations.

The simulation of the 15MA ITER Q ~10 scenario described in [Lukash EPS 2014, Parail NF 2013] was re-assessed in iterations with the JINTRAC code suite to model plasma transport for the fastest plasma current ramp-up (lasting ~50 s) in ITER, which is limited by the voltage produced by the power supply of the central solenoid central module (CS1), followed by the L-H transition and density ramp to stationary high Q burning flat-top conditions, as well as the ramp-down phase including the back transition to L-mode with transport model assumptions as described in [Romanelli NF 2015] and recently validated for

transient JET plasma regimes [Koechl NF 2017, Koechl PPCF 2018], respecting boundary conditions required for robust divertor operation [Militello-Asp FEC 2016]. All simulations are carried out fully predictively solving transport equations for q, pe, pi, nD, nT, vtor and densities for all impurity ionisation states. He ash transport and Ne seeding for control of divertor power loads are included in the transport calculations in phases with significant concentrations in He and Ne, while Be transport is considered otherwise. Neoclassical transport is modelled with NCLASS [Houlberg PoP 1997] and turbulent transport is described by the L-mode version of the Bohm-gyroBohm model in L-mode [Erba JET-R 1996] or by the GLF23 [Waltz PoP 1997] model in H-mode, unless stated otherwise.

## 3. Benchmark results for the IMAS DINA-JINTRAC coupling scheme

Attempts were made to verify that the solutions for the confined region obtained by the equilibrium solver and the current diffusion equation in DINA vs. JINTRAC are in reasonable agreement for the same boundary conditions which is a crucial requirement for the DINA-JINTRAC coupling scheme to ensure convergence at high accuracy. The same sequence of kinetic and non-inductive current density profiles has been applied and the same assumptions were made for the plasma boundary shape and total current evolution in both codes in dedicated test simulations for the current ramp-up phase. Results for the RMS deviation in  $\Psi_{\text{norm}}(R,Z)$  evaluated on the outer and inner mid-plane and for the deviation in  $|\Psi_{\text{axis}}-\Psi_{\text{sep}}|$  are shown in Fig. 1. Apart from the early ramp-up phase which is influenced by different initial conditions for the current diffusion equation at the start of the simulation, the differences in the solutions are found to remain in the order of ~1% which agrees with the expected error in the solution due to interpolation errors, differences in the time resolution for the prescription of kinetic profiles, and limited resolution for the description of the boundary contour (~100 contour points in JINTRAC) and the 2D (R,Z) grid used for the solution of the GS equation (~10<sup>4</sup> points in both codes).

This result confirms that the solutions obtained in both codes can indeed be considered as identical for the same boundary conditions within given resolution dependent tolerances. It can be considered as a verification of the implementation of the GS equation solver and the current diffusion equation in both codes and it may also serve as a confirmation of the correct definition and interpretation of IMAS IDS I/O structures (e.g. equilibrium, core\_profiles, core\_sources, adhering to COCOS=11 standard [Sauter CPC 2013]) used in the DINA-JINTRAC core+edge simulations.

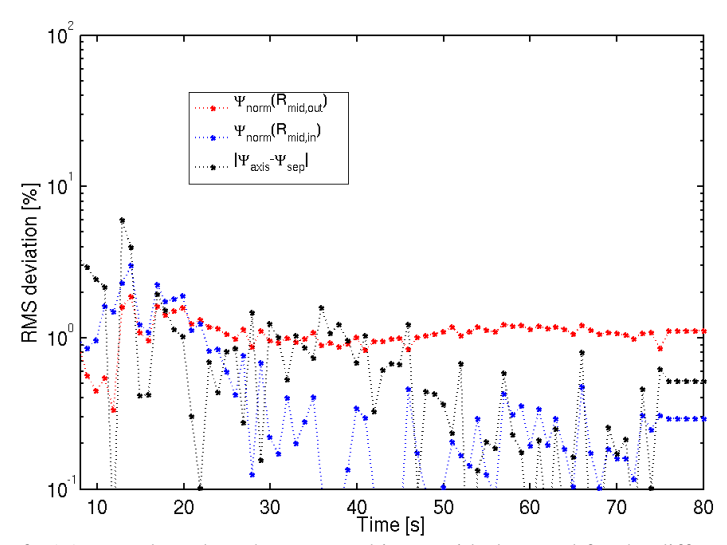


Figure 1. RMS deviation for  $\Psi_{norm}$  evaluated on the outer and inner mid-plane and for the difference in  $\Psi$  between the axis and separatrix, comparing the  $\Psi$  solution obtained by the GS solvers in DINA and JINTRAC with the same prescribed

kinetic and non-inductive current density profiles and boundary conditions for the current ramp-up phase of the ITER baseline scenario.

### 4. Complete baseline scenario investigation with DINA+JINTRAC IMAS workflow

Simulation results obtained for the initial iteration with the DINA+JINTRAC IMAS core+edge transport workflow indicate that, due to the low value of the plasma internal inductance  $(l_i)$  during the ramp-up phase in this scenario, the maximum value of the magnetic field on the PF6 coil conductor  $(max(B_{PF6}))$ , is significantly higher than its design limit (7.3 T vs. 6.4 T). Increasing the ramp-up duration to 70 s was found to be sufficient to reduce max(B<sub>PF6</sub>) down to its design limit of 6.4 T. Further increase of the ramp-up duration to 80 s led to a reduction in  $max(B_{PF6})$  to 6.1 T. The DINA+JINTRAC modelling confirms that for a ramp-up duration of 70 s the PF system can support a burn length duration of ~660 s, whereas for 80 s the burn duration is reduced to ~500 s, although this is dependent on the achieved core impurity concentration during the burn. In the simulations with 70 s and 80 s of the ramp-up duration all engineering parameters are within the limits. In the following iterations, a ramp-up duration of 75 s has been selected as a compromise between burn length maximisation and  $B_{PF6}$  optimisation. The ramp-down phase has also been optimised in the next iteration in order to improve vertical stability, plasma density evolution, as well as the control of W sputtering and divertor power loads along recent findings discussed in [Poli FEC 2018].

Time traces for the main phases of interest for the first and second iterations are shown in Figs. 2-3, demonstrating that simulations converge very quickly, i.e. the same solution is obtained in both codes within an error margin of ~1%, and the deviation in simulation results between two consecutive iterations also approaches a level of 1%. These conditions are fulfilled after the third iteration. Without adaptations of the scenario conditions that have been applied after the first iteration, convergence could even be achieved within two iterations. Due to the low number of iterations required, a fully converged solution for the whole scenario may typically be obtained with the DINA+JINTRAC IMAS core+edge transport workflow on the ITER HPC cluster within a time of two weeks.

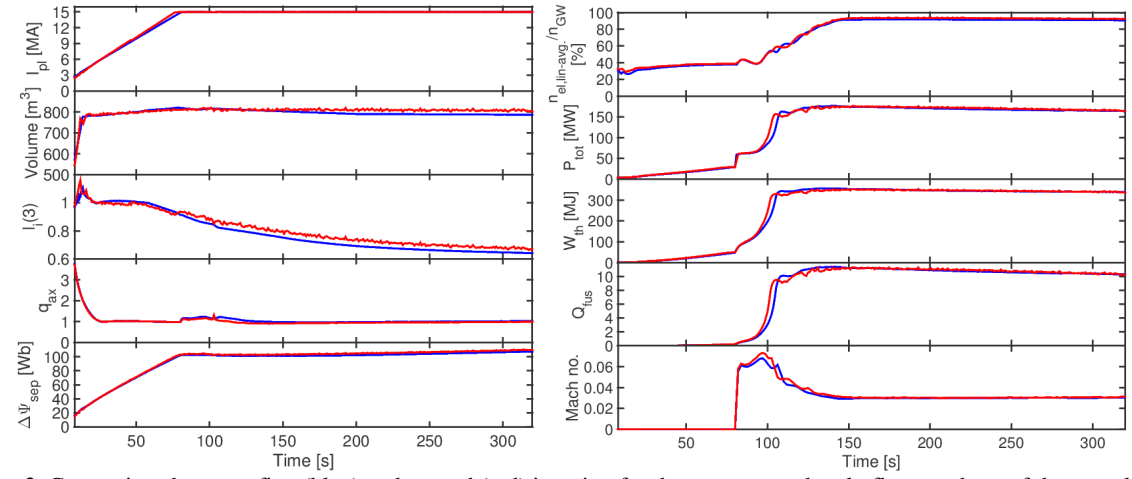


**Figure 2.** Comparison between first (blue) and second (red) iteration for the ramp-up and early flat-top phase of the complete ITER DT 15 MA/5.3 T baseline scenario calculation with the IMAS DINA-JINTRAC workflow. Left, from top to bottom: Total plasma current, plasma volume, internal inductance  $l_i(3)$ , safety factor on axis, poloidal flux variation at the separatrix, right, from top to bottom: Greenwald density fraction, total input power, thermal energy content, fusion Q, Mach number for toroidal rotation on axis. Deviations in time traces are mainly triggered by minor adjustments in scenario conditions for optimisation after the first iteration (ramp-up duration reduced from 80 to 75 s, slightly delayed start of H-mode after ramp-up). Full convergence is achieved after the third iteration with fixed scenario conditions.

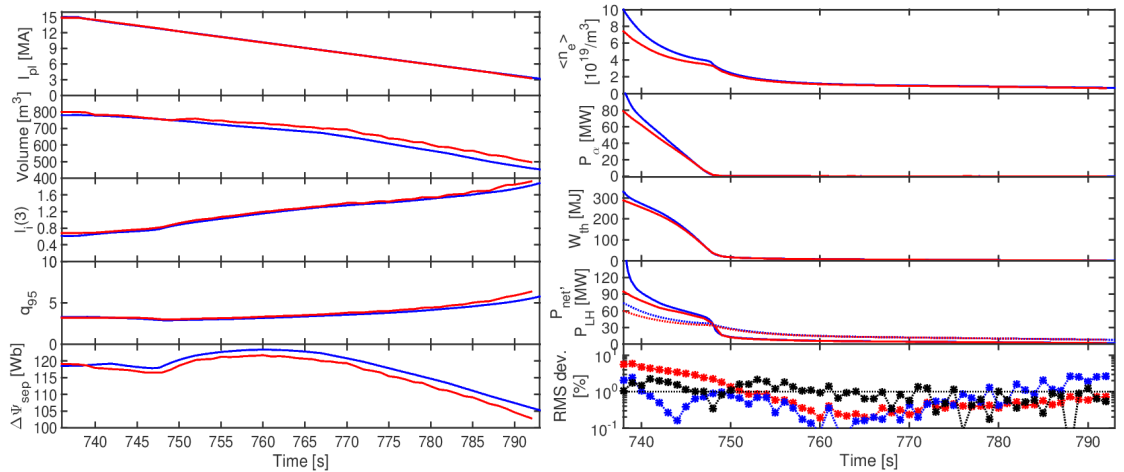
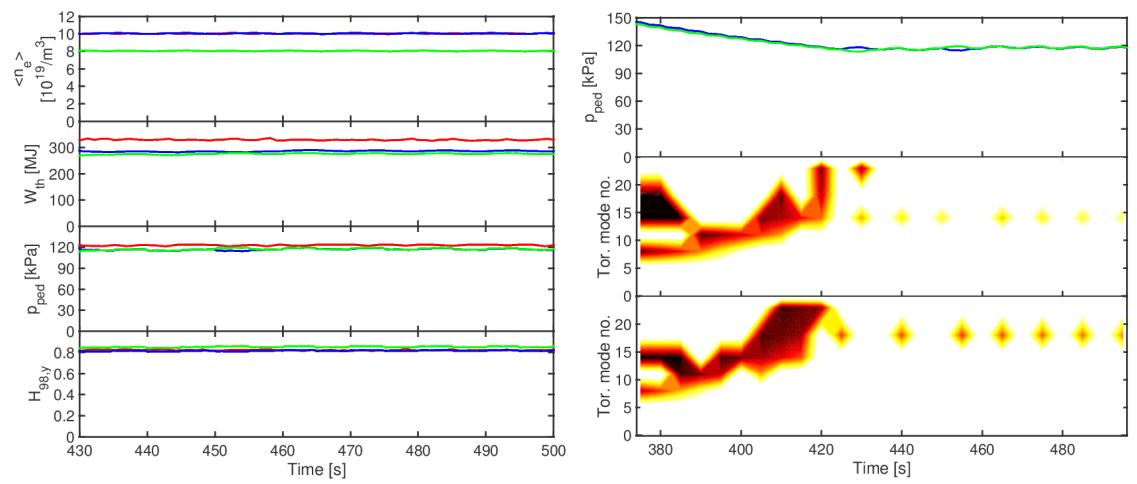


Figure 3. Comparison between first (blue) and second (red) iteration for the current ramp-down phase of the complete ITER DT 15 MA / 5.3 T baseline scenario calculation with the IMAS DINA-JINTRAC workflow. Left, from top to bottom: Total plasma current, plasma volume, internal inductance  $l_i(3)$ , safety factor on axis, poloidal flux variation at the separatrix, right, from top to bottom: volume averaged electron density, alpha power, thermal energy content, net heat flux  $P_{net}$  (solid) vs. L-H transition threshold power  $P_{L-H}$ , RMS deviation in  $\Psi_{norm}$  evaluated at the outer (red) and inner (blue) mid-plane and relative difference in  $|\Psi_{ax}^{-}\Psi_{sep}|$  (black). Deviations in time traces are mainly triggered by minor adjustments in scenario conditions for optimisation after the first iteration (delayed start of ramp-down with respect to time of removal of fuelling and auxiliary heating, improved plasma stability and shape control strategy). Full convergence may be achieved after the third iteration with fixed scenario conditions.

# 5. Free boundary core+edge+MHD ITER baseline scenario assessment with DINA+JINTRAC IMAS workflow

In the simulations presented in the previous section, the continuous ELM model [Parail NF 2009] has been applied to keep the maximum normalised pedestal gradient within the ETB close to a prescribed threshold  $\alpha_{crit}$ , which needs to be inferred from external MHD stability calculations which may not be fully consistent with the plasma conditions considered in the DINA+JINTRAC runs. The IMAS DINA+JINTRAC workflow has therefore been adapted such that simulations can be run with ongoing checks of the MHD edge stability by exploitation of a coupling to the HELENA+MISHKA codes [Mikhailovskii PPR 1997] within JINTRAC.  $\alpha_{crit}$  can then be regularly adjusted in time in accordance with the results obtained from the MHD stability calculations.

For the ITER baseline scenario, first free boundary core+edge+MHD simulations have been carried out with this scheme with DINA+JINTRAC based on the runs presented in the previous section. Instead of GLF23, the Weiland model based EDWM model [Strand EPS 2004] has been used for the prediction of anomalous core transport in these runs. HELENA+MISHKA is called every  $\sim$ 3-5 s in the flat-top phase and  $\alpha_{crit}$  is updated each time such that the pedestal pressure gradient remains close to the MHD stability limit while P<sub>net</sub>/P<sub>L</sub>- $_{\rm H} >> 1$ . A comparison of the predicted pedestal pressure  $p_{\rm ped}$  and associated quantities with the results obtained in the runs presented in the previous section, in which pped was determined by a scaling derived from EPED1+SOLPS calculations [Polevoi NF 2015], shows that results obtained for edge MHD stability are in close agreement. This result may not be surprising as the boundary conditions applied in these runs for the density and temperature at the separatrix are the same as those used in the derivation of the EPED1+SOLPS scaling, and the ETB width is determined by the same scaling as given in [Polevoi NF 2015]. On the other hand, assumptions for the core confinement may not be identical. With EDWM,  $Q_{fus} \sim 7$  is achieved in the late flattop phase, but predictions may be conservative as electromagnetic effects which might cause a slight improvement in confinement have not been taken into account.



**Figure 4.** Left: Comparison between simulations of the later flat-top phase of the ITER baseline scenario with DINA+JINTRAC and automatic adjustment of  $\alpha_{crit,ETB}$  in accordance with regular MHD stability calculations with HELENA+MISHKA, at ~90% (blue) and ~70% (green) of the Greenwald density with the DINA+JINTRAC simulation with pedestal conditions determined by the EPED1+SOLPS scaling (red, same case as shown in the previous section). From top to bottom:  $\langle n_e \rangle$ , thermal energy content, pressure on top of the pedestal,  $H_{98,y}$ . Right: similar cases as shown in the left figure with automatic adjustment of  $\alpha_{crit,ETB}$ , but re-initialising the simulation at t ~ 375 s with artificially increased pedestal pressure to demonstrate the reaction of the  $\alpha_{crit,ETB}$  control scheme with HELENA+MISHKA. Top: pedestal pressure for cases at ~90% (blue) and ~70% (green) of the Greenwald density, middle / bottom: contour plots of growth rates in a.u. as function of toroidal modes indicating toroidal modes found to be marginally unstable by HELENA+MISHKA for the cases at ~90% (middle) and ~70% (bottom) of the Greenwald density.

# 6. First free boundary core+edge+SOL+MHD simulations with DINA+JINTRAC IMAS workflow

In an attempt to extend the level of integration by combination of the new capabilities for integrated modelling with the IMAS DINA+JINTRAC workflow, the HELENA+MISHKA coupling for the assessment of edge MHD stability and the coupling of the core+edge transport codes JETTO+SANCO with the SOL transport and plasma wall interaction codes EDGE2D+EIRENE within JINTRAC, first free boundary core+edge+SOL+MHD modelling studies have been carried out for the ramp-up and early flattop phases as well as for the rampdown phase of the ITER baseline scenario based on core+edge+SOL JINTRAC calculations presented in [Militello-Asp NF 2019]. In addition to the IMAS coupling scheme that is also applied in the DINA+JINTRAC core+edge transport calculations as summarised in Section 4, information for the time-evolving 2D SOL grid is retrieved from the equilibrium IDS structure of the DINA output and imposed in JINTRAC. While the procedure for the preparation of the set of 2D SOL grids is not yet fully automatised and needs to be carried out offline, JINTRAC can now be run with time-evolving SOL grids without manual intervention. Results for the first two iterations between DINA and JINTRAC are shown in Fig. 5 for the ramp-up and early flat-top phases. As indicated by the RMS deviations for the Ψ solutions in Fig. 5b, fast convergence can be achieved despite some changes in simulation assumptions that have been applied in the second iteration (e.g. forced L-mode during low density rampup, slightly deviating assumptions in anomalous ETB transport suppression for P<sub>net</sub> close to P<sub>L-H</sub>, different initial impurity concentration, improved calculation of wall-neutral interactions), and it may be possible to design a scenario configuration for the ITER baseline scenario in which Q~10 can be approached fulfilling all operational constraints. For the first time, it is possible with this modelling scheme to make predictions without the need to impose any boundary conditions within the domain of the plasma vessel. The model predictions depend only on natural external boundary conditions that are either fixed or pre-programmed, such as the vessel wall configuration, wall material, heating, fuelling and pumping conditions as well as coil locations and currents, and the uncertainty of the modelling predictions can be reduced to the uncertainty of the models in use. With this fully integrated modelling scheme, it is now possible to make truly fully consistent predictions of time evolving plasma conditions. In addition, this scheme is also advantageous for the modelling of plasmas in stationary conditions. In the latter case, the modelling can be carried out more efficiently, as no internal boundary conditions need to be defined. That way, detailed investigations to find a proper parameterisation within a large dimension space or extensive sensitivity studies, as they would be required if internal boundary conditions had to be set up, could be avoided.

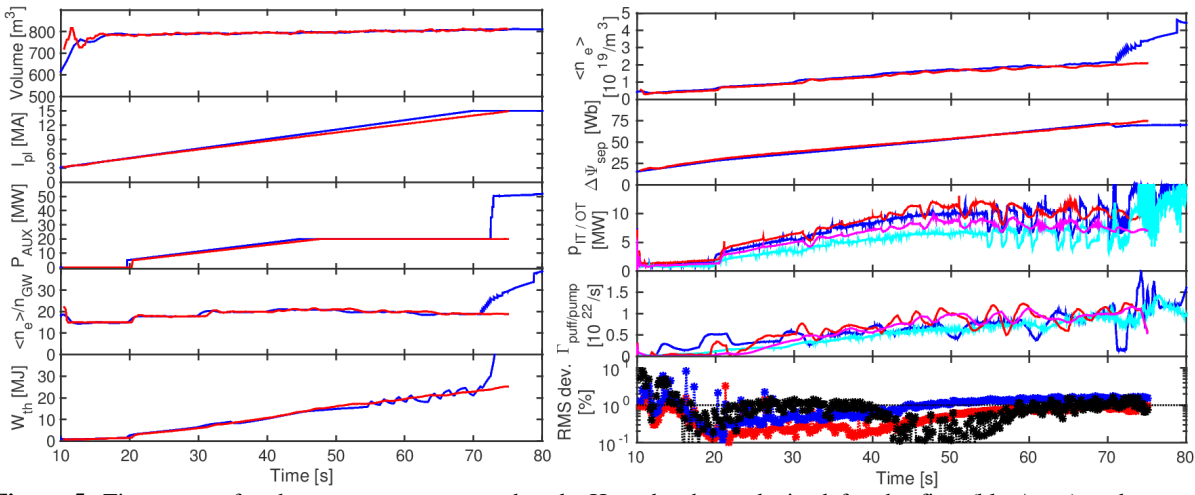


**Figure 5.** Time traces for the current ramp-up and early H-mode phase obtained for the first (blue/cyan) and second (red/magenta) iteration of a free boundary core+edge+SOL+MHD simulation with the IMAS DINA+JINTRAC workflow for the ITER baseline scenario. Left, from top to bottom: plasma volume, plasma current,  $P_{AUX}$ , Greenwald density fraction, thermal energy content. Right, from top to bottom:  $\langle n_e \rangle$ , poloidal flux variation at the separatrix, power deposited on the outer (blue/red) and inner (cyan/magenta) targets (neglecting contributions from radiation and neutral interaction), rates of puffed (blue/red) and pumped (cyan/magenta) DT particles (approximate estimate, smoothed in time), RMS deviation in  $\Psi_{norm}$  evaluated at the outer (red) and inner (blue) mid-plane and relative difference in  $|\Psi_{ax}-\Psi_{sep}|$  (black) obtained in the second iteration. This figure still needs to be updated considering results for the second iteration for the early flat-top phase!

# 7. Assessment of impact of increased medium-Z impurity concentration on H-mode core confinement

As detailed in [Frigione FEC 2018, Romanelli NF 2019], it has been observed in JET experiments, that the presence of an increased concentration in medium-Z impurities may cause an improvement in core confinement that could be associated with enhanced inwardsdirected turbulent particle convection. Similarly, indications for an improvement in confinement that may be linked to a significant increase in impurity concentration have also recently been reported for dedicated ADITYA-U experiments [Chowduri FEC 2018]. The associated mechanism of a damping of ITG modes in case of peaked density profiles and of a stabilising effect through dilution for increased Z<sub>eff</sub> has first been investigated systematically for TEXTOR experiments [Bourdelle NF 2002, Tokar PRL 2000]. It was found to be well reproducible with the QuaLiKiz [Bourdelle PPCF 2016, Citrin PPCF 2017] transport model. Turbulent transport predictions obtained with QuaLiKiz for a scan in Zeff have been successfully validated against non-linear GYRO calculations [Casati NF 2009], and it was possible to reproduce the impurity transport behaviour and confinement improvement observed for increased Z<sub>eff</sub> in Ne scan experiments at JET as described in [Frigione FEC 2018] by means of integrated predictive core+edge transport simulations with QuaLiKiz embedded in JINTRAC [Romanelli NF 2019]. To evaluate to which extent an enhanced core contamination by medium-Z impurities might also lead to improved H-mode confinement in the ITER baseline scenario, DINA-JINTRAC core+edge simulations have been repeated for a short period in the later flat-top phase with QuaLiKiz including ETG scales, but neglecting rotation, with varying edge Ne concentration. Plasma profiles with identical electron density are fixed in time and imposed in these runs for  $\rho_{norm} > 0.85$ . A constant pellet particle source rate of  $\sim 3 \cdot 10^{22}/s$  (for the entire confined region) has been prescribed.

As indicated by the plots in Figs. 6-7, the core density is not predicted to be more peaked as in the JET experiments, however, transport conditions for the ITER baseline scenario cases with high vs. low Ne concentration may not be directly comparable, as the heat source is not the same. Due to increased dilution in the case with high Ne concentration, the alpha power is reduced. In addition, the core radiation is increased. For that reason, the temperature gradients in that case may remain closer to the stiffness threshold than in the case with low Ne concentration, and the amplitude of the turbulence-associated inward pinch may therefore be reduced. Nevertheless, it can be seen by comparison of the predicted thermal energy content, the H<sub>98,y</sub> factor and plasma profiles, that the detrimental impact of an increased presence of Ne due to reduced  $P_{\alpha}$  and increased  $P_{\text{rad}}$  seems to become compensated by an improvement in core transport conditions similar to the one observed in the JET experiments. There may be an optimum case with a medium Ne concentration between the low and high concentration values applied in the two simulations shown in Fig. 6 for which the favourable effect of Ne on transport conditions may already be present but the unfavourable effects may not yet be sizeable which will be investigated in [Romanelli NF 2019]. It should be noted that the core Ne concentration achieved in integrated core+edge+SOL transport modelling studies in [Garzotti NF 2018] for stationary flat-top conditions for the ITER baseline scenario with moderate Ne seeding to maintain a partially attached divertor regime is rather low with Z<sub>eff</sub> ~ 1.3-1.4, and the improvement in core confinement due to the presence of Ne may be marginal. However, due to the possibility to control the SOL and core density separately by means of gas vs. pellet fuelling, it may be possible to conceive a regime with deliberately enhanced Ne seeding rates operating at reduced divertor density to avoid complete divertor detachment due to the increase in Ne radiation in the SOL. The predicted improvement in core confinement with increased Ne seeding seems to scale particularly favourably for DEMO regimes at high radiation.

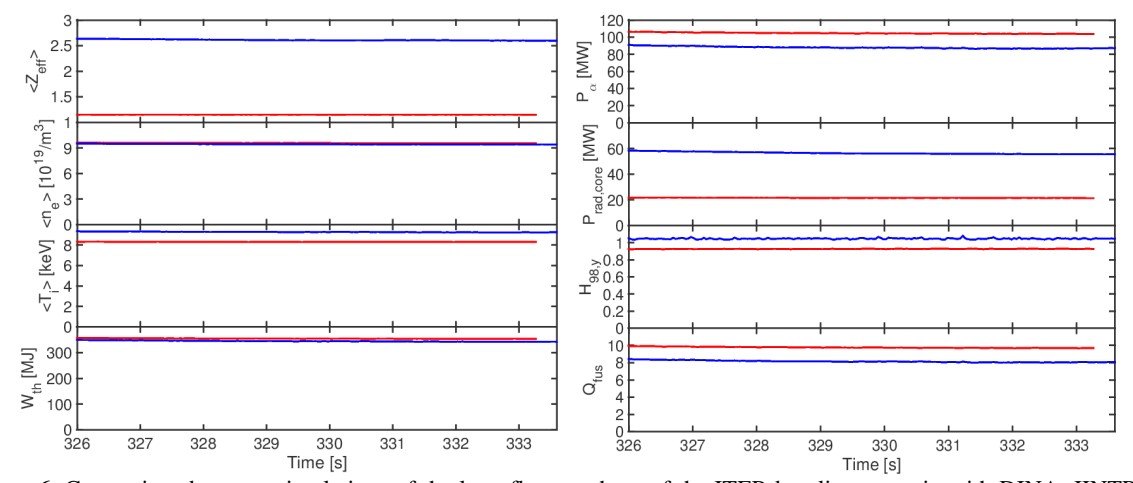


**Figure 6.** Comparison between simulations of the later flat-top phase of the ITER baseline scenario with DINA+JINTRAC and turbulent core transport predicted by QuaLiKiz, for low (red) and high (blue) concentrations of Ne. Left, from top to bottom: Time evolution of  $\langle Z_{eff} \rangle$ ,  $\langle n_e \rangle$ ,  $\langle T_i \rangle$ , thermal energy. Right, from top to bottom:  $P_{\alpha}$ ,  $P_{rad}$ ,  $H_{98,y}$ ,  $Q_{fus}$ .

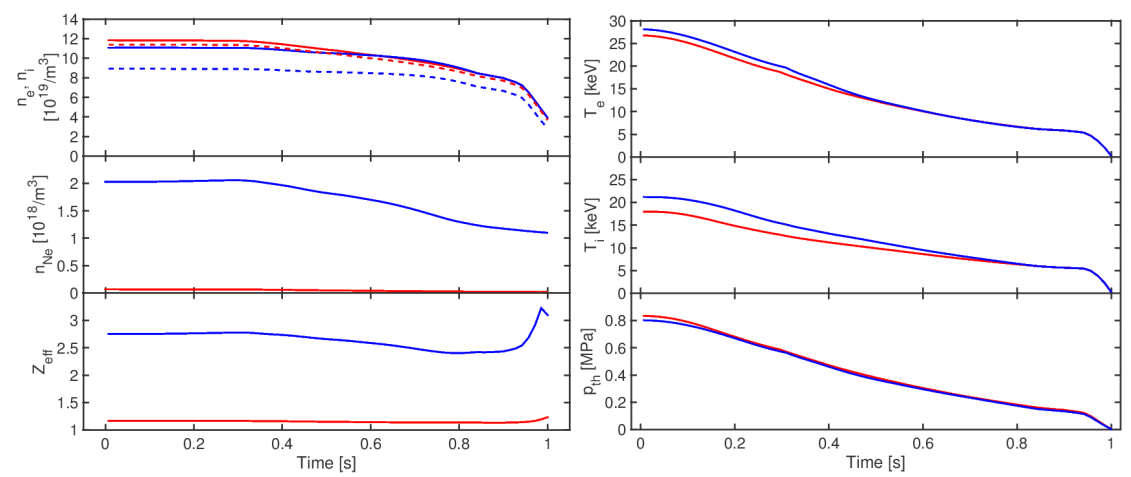


Figure 7. Comparison between simulations of the later flat-top phase of the ITER baseline scenario with DINA+JINTRAC and turbulent core transport predicted by QuaLiKiz, for low (red) and high (blue) concentrations of Ne. Left, from top to bottom: electron (solid) and ion (dashed) density, Ne density and  $Z_{\rm eff}$ . Right, from top to bottom: Electron temperature, ion temperature, thermal pressure.

#### 8. Conclusions

A new IMAS modelling workflow for the fast execution of highly integrated DINA+JINTRAC simulations has been described and applied for the assessment and optimisation of the ITER 15 MA DT baseline scenario. Conclusions have been drawn regarding the available operational space and control capabilities. Benchmark results have been shown confirming that the same solution for the equilibrium and current diffusion is obtained in DINA and JINTRAC within the expected error range due to limited resolution. For stationary conditions and slow transients including the current ramp, L-H and H-L transition phases, the IMAS DINA+JINTRAC simulations were found to converge within only ~2-3 iterations. The modelling scheme has been extended to include the possibility to consistently determine the MHD limit for the pedestal pressure gradient in the simulation in accordance with MHD stability calculations carried out on the fly with HELENA+MISHKA, and it has been extended to core+edge+SOL coupled transport calculations with JETTO+SANCO coupled to EDGE2D+EIRENE with a time-evolving 2D SOL grid derived from the DINA equilibrium. It could be shown that a robust execution of the baseline scenario discharge can be assured by means of optimisation of the scenario design with plasma conditions being well within operational limits at all times. For the optimisation of core impurity control, complementary modelling studies have been carried out for the flat-top phase of the ITER baseline scenario assessing the impact of improved core transport conditions due to the presence of medium-Z impurities.

## Acknowledgements

The views and opinions expressed herein do not necessarily reflect those of the ITER Organization. This work has been partly carried out within the framework of the EUROfusion Consortium and has received funding from the Euratom research and training programme 2014-2018 under grant agreement No 633053 and from the RCUK Energy Programme [grant number EP/I501045]. To obtain further information on the data and models underlying this paper please contact PublicationsManager@ccfe.ac.uk. The views and opinions expressed herein do not necessarily reflect those of the European Commission.

### References

[Bourdelle PPCF 2016] Bourdelle, C. et al., Plasma Phys. Control. Fusion **58** (2016) 14036 [Bourdelle NF 2002] Bourdelle, C. et al., Nucl. Fusion **42** (2002) 892

[Casati NF 2009] Casati A. et al. Nucl. Fusion 49 (2009) 085012 [Chowduri FEC 2018] Chowduri, M. B. et al. Proc. 27th IAEA FEC, Ahmedabad, India, 2018, paper EX/P4-5 (https://nucleus.iaea.org/sites/fusionportal/Shared%20Documents/FEC%202018/fec20 18-preprints/preprint0578.pdf) [Citrin PPCF 2017] Citrin, J. et al., Plasma Phys. Control. Fusion 59 (2017) 124005 [Erba JET-R 1996] Erba, M. et al., JET Report JET-R(96)07 (1996) [Frigione FEC 2018] Frigione, D. et al. Proc. 27th IAEA FEC, Ahmedabad, India, 2018, paper EX/P1-3 (https://nucleus.iaea.org/sites/fusionportal/Shared%20Documents/FEC%202018/fec20 18-preprints/preprint0233.pdf) [Garzotti NF 2018] Garzotti, L. et al., Nucl. Fusion 59 (2019) 026006 [Houlberg PoP 1997] Houlberg, W.A. et al., Phys. Plasmas 4 (1997) 3230 [Imbeaux NF 2015] Imbeaux, F. et al., Nucl. Fusion 55 (2015) 123006 Koechl, F. et al., Nucl. Fusion 57 (2017) 086023 [Koechl NF 2017] [Koechl PPCF 2018] Koechl, F. et al., Plasma Phys. Control. Fusion 60 (2018) 074008 Lukash, V. E. et al 2011 Proc. 38th EPS Conf. on Plasma Physics (Strasbourg, France, [Lukash EPS 2011] 27 June - 1 July 2011) vol 35G P2.109 (http://ocs.ciemat.es/EPS2011PAP/pdf/P2.109.pdf) [Lukash EPS 2014] Lukash, V. E. et al 2014 Proc. 41st EPS Conf. on Plasma Physics (Berlin, Germany, 23-27 June 2014) vol 38F P5.010 (http://ocs.ciemat.es/EPS2014PAP/pdf/P5.010.pdf) Lukash, V. E. et al., Plasma Devices and Operations 13 No.2 (2005) 143 [Lukash PDO 2005] [Mikhailovskii PPR 1997] Mikhailovskii, A. B. et al., Plasma Phys. Rep. 23 (1997) 713 [Militello-Asp FEC 2016] Militello-Asp, E. et al., Proc. 26th IAEA FEC, Kyoto, Japan, 2016, paper TH/P2-23 (https://nucleus.iaea.org/sites/fusionportal/Shared%20Documents/FEC%202016/fec20 16-preprints/preprint0255.pdf) [Militello-Asp NF 2019] Militello-Asp, E., "JINTRAC Coupled Core/SOL/Divertor Transport Simulations in Support of ITER", submitted to Nucl. Fusion [Parail NF 2009] Parail, V. et al., Nucl. Fusion 49 (2009) 075030 [Parail NF 2013] Parail, V. et al., Nucl. Fusion 53 (2013) 113002 Pinches, S. D. et al., Proc. 26th IAEA FEC, Kyoto, Japan, 2016, paper TH/P2-14 [Pinches FEC 2016] (https://nucleus.iaea.org/sites/fusionportal/Shared%20Documents/FEC%202016/fec20 16-preprints/preprint0518.pdf) Polevoi, A.R. et al., Nucl. Fusion 55 (2015) 063019 [Polevoi NF 2015] [Poli FEC 2018] Poli, F. et al., Proc. 27th IAEA FEC, Ahmedabad, India, 2018, paper EX/P7-27 (https://nucleus.iaea.org/sites/fusionportal/Shared%20Documents/FEC%202018/fec20 18-preprints/preprint0295.pdf) [Romanelli NF 2015] Romanelli, M. et al., Nucl. Fusion 55 (2015) 093008 [Romanelli NF 2019] Romanelli, M. et al., "Electron Density Peaking Induced by Ne Seeding in JET Hybrid Plasmas", 23rd Joint EU-US Transport Task Force Meeting (Seville, Spain, 11-14 September 2018), to be submitted to Nucl. Fusion [Romanelli PFR 2014] Romanelli, M. et al., Plasma and Fusion Research 9 (2014) 3403023 [Sauter CPC 2013] Sauter, O. and Medvedev, S. Yu., Comp. Phys. Comm. 184 (2013) 293-302 [Strand EPS 2004] Strand P. et al. 2004 Proc. 31th EPS Conf. on Plasma Physics (London, UK, 28 June -2 July 2004) vol 28G P5.187 (http://epsppd.epfl.ch/London/pdf/P5\_187.pdf) Tokar, M. Z. et al., Phys. Rev. Lett. 84 (2000) 895 [Tokar PRL 2000] [Waltz PoP 1997] Waltz, R.E. et al., Phys. Plasmas 4 (1997) 2482